frontiers | Frontiers in Environmental Science

TYPE Original Research
PUBLISHED 25 September 2025
DOI 10.3389/fenvs.2025.1615267

OPEN ACCESS

EDITED BY
Yang Song,
University of Michigan, United States

REVIEWED BY
Michael Pollock,
Northwest Fisheries Science Center, NOAA Fisheries, United States
Terry Eugene Whitledge,
Retired, Fairbanks, AK, United States

*CORRESPONDENCE
Haojun Deng,
denghaojun1990@zqu.edu.cn
Qun Cai,
caiqun1991@126.com

RECEIVED 21 April 2025
ACCEPTED 09 September 2025
PUBLISHED 25 September 2025

CITATION
Deng H, Zheng Z, Cai Q, Wu J and Chen A (2025) Spatial and temporal dynamics of phytoplankton primary productivity in Chinese reservoirs: influencing factors and carbon sequestration.
Front. Environ. Sci. 13:1615267.
doi: 10.3389/fenvs.2025.1615267

Spatial and temporal dynamics of phytoplankton primary productivity in Chinese reservoirs: influencing factors and carbon sequestration

Haojun Deng[1]*, Zhuangpeng Zheng[1], Qun Cai[1]*, Jingyi Wu[1] and Aimin Chen[2]

[1]School of Tourism and Historical Culture, Zhaoqing University, Zhaoqing, Guangdong, China, [2]School of Environment and Tourism, West Anhui University, Lu'an, China

Phytoplankton primary production (PP) underpins the sustainability of aquatic ecosystems in reservoirs. However, national-scale studies of reservoir phytoplankton PP in China remain limited, typically subsumed within lake research, hindering mechanistic understanding of large-scale PP variations. To address this gap, we compiled a database of phytoplankton PP in Chinese reservoirs (1980–2023) based on an exhaustive literature review, incorporating only data measured using the light-dark bottle method. Utilizing this database, this study quantifies phytoplankton PP and carbon sequestration potential across 165 Chinese reservoirs. The result showed that phytoplankton PP ranged 0.13–10.22 g $O_2 \cdot m^{-2} \cdot d^{-1}$, with significantly higher values in the Yellow River (YR), Songhua River and Liaohe River (S/LR), and Haihe and Huaihe River (H/HR) basins versus the Pearl River (PR), Northwest Internal Rivers (NIR), and Southwest Rivers (SWR) basins. Temporally, phytoplankton PP peaked in the 1990s, declined thereafter, but rebounded in the 2020s (decadal sequence: 1990s > 2020s > 2000s > 1980s > 2010s). Seasonal variation followed summer > spring > autumn > winter. Sunshine hours, water depth, and rainfall emerged as dominant phytoplankton PP drivers. National phytoplankton PP extrapolation reached 22.08 $Tg \cdot O_2 \cdot a^{-1}$ (1 Tg = 10^{12} g), equivalent to 6.62 Tg carbon sequestration capacity. Our analysis delineates spatio-temporal patterns of phytoplankton PP in Chinese reservoirs and underscores its significance for regional carbon budgets and aquatic ecosystem dynamics.

KEYWORDS

phytoplankton primary productivity, temporal and spatial variations, influencing factors, carbon sequestration, Chinese reservoirs

1 Introduction

Intensifying industrialization and urbanization underscore the global imperative to mitigate carbon emissions and enhance carbon sinks (Wang et al., 2024). Quantifying carbon sequestration capacities across terrestrial and aquatic ecosystems is critical for offsetting industrial greenhouse gases (Jia et al., 2023). Satellite data since 1980 reveal increasing phytoplankton bloom frequency in global lakes/reservoirs (Ho et al., 2019), signaling significant primary productivity shifts. Such alterations may disrupt aquatic ecosystem dynamics, impair service provision, and threaten system sustainability (Sun et al.,

2023). Within the global aquatic carbon cycle, phytoplankton plays an instrumental role in primary production (PP) due to their ability to sequester carbon dioxide. Globally, recent studies estimate that phytoplankton sequester in global inland lakes approximately 1.77 Pg C annually (Gao et al., 2021), highlighting their pivotal role in carbon sink processes across aquatic.

Phytoplankton absorb essential nutrients and, through chlorophyll-driven photosynthesis, produce oxygen while transferring energy to other organisms (Zhang et al., 2016; Rusanov et al., 2022). Phytoplankton are sensitive indicators of physical and chemical changes in aquatic environments (Wei et al., 2024). Their diversity and community structure reflect alterations in water quality (Xiao et al., 2018) and directly influence ecologically and economically important species (Essa et al., 2024). Shifts in phytoplankton communities signal environmental disturbances within watersheds (Wei et al., 2022). Therefore, analyzing phytoplankton responses to physicochemical changes is essential for assessing reservoir water quality and understanding how community structure affects eutrophication (Wagner and Erickson, 2017; Yu et al., 2022; Ruan et al., 2024).

More than 16 million dams have been constructed globally, with over 50,000 standing taller than 15 m (Berga et al., 2006; Lehner et al., 2011). Primarily built for hydropower, these dams substantially disrupt river ecosystems and alter organic carbon fluxes to oceans (Yi et al., 2022). Such large-scale modifications complicate biogeochemical cycles, particularly organic carbon transport and fate (Carey and Fulweiler, 2012; Hughes et al., 2012; Grill et al., 2019). Driven by economic growth and rising energy/food demands since the 1980s, China's rapid dam development added over 15,000 reservoirs (Ran et al., 2021). This expanded the water surface area from 14,772 km^2 (1980s) to 25,616 km^2 (2010s) and more than doubled total storage capacity (Ran et al., 2021).

Sun et al. (2023) developed the vertically generalized production model (VGPM) using long-term multi-site water quality data. This framework estimated annual phytoplankton carbon sequestration in Chinese lakes/reservoirs at 18.69 ± 10.7 Tg C (1 Tg = 10^{12} g), identifying chlorophyll, nitrogen, phosphorus, and turbidity as key determinants. Phytoplankton PP in inland waters is governed by community composition, biomass, and environmental variables (nutrients, light, temperature, Secchi depth) (Zhang et al., 2016; Hiroki et al., 2020; Rusanov et al., 2022; Jung et al., 2023). Reservoir PP exhibits distinct transitional characteristics between rivers and lakes, correlating strongly with seasonal discharge and anthropogenic regulation (Ran et al., 2016; Han et al., 2018). Nevertheless, national-scale studies of reservoir PP in China remain limited, typically subsumed within lake research (Ran et al., 2013b; Gao et al., 2018; Deng et al., 2020; Jia et al., 2020; Sun et al., 2023), hindering mechanistic understanding of large-scale PP variations.

Primary methods for estimating phytoplankton PP include: light-dark bottle incubation, VGPM, and carbon isotope techniques (Pratt and Berkson, 1959; Cox et al., 2015; Lan et al., 2020; Lu et al., 2023). Comprehensive spatiotemporal PP data remain limited by regional sampling constraints (Sun et al., 2023). Though often overlooked in carbon capture studies, the light-dark bottle method provides critical historical baselines for evaluating long-term PP trends (Hiroki et al., 2020). This study integrates public reservoir PP data obtained via this methodology to: (1) characterize fundamental phytoplankton PP features in Chinese reservoirs; (2) identify key influencing factors; and (3) estimate the sequestration of organic carbon by phytoplankton.

2 Materials and methods

2.1 Data sources

An exhaustive search and examination of all literature on phytoplankton PP in Chinese reservoirs from 1980 to 2023 was conducted using the China Knowledge Network Database and Web of Science. Information such as phytoplankton PP, geographical coordinates (latitude and longitude), sunshine hours, Secchi depth (SD), reservoir age, storage capacity, mean water depth, reservoir area, annual average temperature, annual average rainfall, total nitrogen (TN), and total phosphorus (TP) was extracted. In addition, the nitrogen-to-phosphorus ratio, water retention time and light limitation index were calculated. A comprehensive database comprising 165 reservoirs was ultimately established (Table 1 and Supplementary Material S1). Reservoir distributions and river basin divisions are shown in Figure 1.

2.2 Data calculation

The light limitation was derived from either photosynthetically active radiation or *in situ* light profile data. The light limitation index was calculated as the ratio of euphotic zone depth (Z_{eu}) and mean water depth Formulas 1,2:

$$Light\ limitation\ index = \frac{Z_{eu}}{water\ depth} \tag{1}$$

$$Z_{eu} = 2.5 \times SD \tag{2}$$

where SD was Secchi depth, the coefficient of 2.5 follows established practice for converting transparency measurements to euphotic depth (Kirk, 1994).

The total phytoplankton PP in Chinese reservoirs was calculated using a simple extrapolation method (Formulas 3,4). Using the photosynthetic principle that 1 mg of O_2 release corresponds to 0.30 mg of organic carbon production, and the carbon sequestration capacity (CSC) formula is as follows (Shiying, 1981):

$$T_{pp} = \sum_{T_{basin}} \left(P \times S \times 365 \times 10^{-9}\right) \tag{3}$$

$$CSC = T_{pp} \times 0.30 \tag{4}$$

where T_{pp} is the aggregate phytoplankton PP in reservoirs nationwide (expressed in Tg $O_2 \cdot a^{-1}$), while P is the median phytoplankton PP within individual basins (in g $O_2 \cdot m^{-2} \cdot d^{-1}$). In addition, S is the surface area of reservoirs within each basin (km^2). The country's total phytoplankton PP is derived by aggregating the individual PP values from all basins. Reservoir surface area data, derived from Ran et al. (2021)and Zhou et al. (2024), were obtained by integrating satellite imagery with national inventories to estimate reservoir surface area and reduce associated uncertainties.

TABLE 1 Characteristics of Reservoir influence factors in different basin.

Factors	Basin							
	S/LR	YR	H/HR	YTZ	PR	NIR	SWR	Average
Secchi depth (cm)	87.6 (14.54)	129 (5.29)	74.97 (11.97)	127.39 (9.62)	35.62 (17.49)	13.94 (13.94)	184 (42)	96.73 (6.58)
Reservoir age (a)	19.89 (1.87)	22.67 (2.33)	23.83 (3.32)	20.59 (1.78)	18.71 (2.57)	19.67 (19.67)	11 (6.24)	20.64 (1.14)
Reservoir capacity (10^8 m^3)	47.21 (41.88)	24.12 (16.44)	1.73 (0.71)	16.21 (7.35)	5.62 (2.07)	0.01 (0.01)	145.14 (75.67)	21 (9.57)
Water depth (m)	3.34 (1.11)	3.17 (3.17)	2.68 (0.3)	6.94 (1.27)	7.32 (3.46)	1.63 (0.82)	—	5.16 (0.75)
Annual discharge (10^8 $m^3 \cdot a^{-1}$)	4.32 (2.16)	96.72 (88.15)	0.69 (0.47)	72.37 (60.88)	3.35 (0.9)	—	418.67 (65.13)	41.54 (26.23)
Reservoir area (km^2)	31.71 (11.11)	56.73 (25.13)	6.38 (3.2)	49.99 (22.45)	23.58 (9.57)	—	64.66 (64.66)	34.3 (10)
Retention time (a)	0.74 (0.19)	0.68 (0.25)	0.18 (0.11)	0.73 (0.15)	0.86 (0.26)	—	0.88 (0.54)	0.64 (0.09)
Total nitrogen ($mg \cdot L^{-1}$)	1.67 (0.17)	1.91 (0.7)	1.05 (0.12)	1.04 (0.06)	0.52 (0.09)	1.26 (0.64)	1.13 (0.38)	1.13 (0.06)
Total phosphorus ($mg \cdot L^{-1}$)	0.21 (0.06)	0.08 (0.03)	0.14 (0.02)	0.07 (0.02)	0.06 (0.01)	0.1 (0.08)	0.17 (0.14)	0.11 (0.02)
N:P ratio	24.71 (4.8)	24.09 (3.7)	10.14 (1.29)	27.22 (2.51)	11.47 (2.72)	11.76 (7.94)	19.12 (7.81)	21.09 (1.63)
Annual average temperature (°C)	5.61 (0.44)	10.47 (1.99)	15.29 (0.19)	16.54 (0.14)	21.12 (0.4)	8.8 (0.72)	19.43 (0.24)	14.43 (0.41)
Annual average precipitation (mm)	648.35 (24)	468.33 (95.4)	872.8 (31.11)	1,051.42 (31.39)	1,648.71 (92.86)	182.67 (43.56)	1,096 (44.26)	985.92 (31.49)
Sunshine hours ($hours \cdot a^{-1}$)	2,479.29 (30.48)	2,500.67 (49.70)	1956.33 (27.90)	1799.20 (21.86)	1,668.665 (25.59)	2,869.33 (109.95)	2087.33 (13.94)	1991.12 (27.66)
Light limitation index	0.47 (0.15)	—	0.86 (0.15)	0.70 (0.17)	0.27 (0.14)	—	—	0.70 (0.10)

Mean (SE); -, no data. All reservoirs are categorized into seven major basins, including the Songhua River and Liaohe River (S/LR) basin, the Haihe and Huaihe River (H/HR) basin, the Yellow River (YR) basin, the Yangtze River (YTZ) basin, the Pearl River (PR) basin, the southwest rivers (SWR) basin and the northwest internal rivers (NIR) basin (Zhou et al., 2024).

2.3 Statistical analysis

The statistical analyses and data plotting were performed using SPSS 18.0, Origin 2019, and ArcGIS 10.7, with a significance threshold of $P < 0.05$ for both difference and correlation evaluations. Descriptive statistics, presented as Mean ± SE, were employed to assess seasonal fluctuations in key indicators and discern differences across reservoirs within various basins. A one-way ANOVA, complemented by the Duncan test, was applied to evaluate variations in phytoplankton PP and seasons. Crucial indicators over distinct decades (1980s, 1990s, 2000s, 2010s, and 2020s) was used Mann-Kendall test. Pearson correlation analysis was conducted to clarify associations between phytoplankton PP and environmental factors. In addition, stepwise multiple regression analysis was utilized to identify the predominant factors influencing phytoplankton PP.

3 Results

3.1 Spatial differentiation of phytoplankton PP in Chinese reservoirs

Data on phytoplankton PP in Chinese reservoirs is predominantly concentrated in the eastern region, with limited observations from the northwest and southwest (Figures 1, 2). The mean phytoplankton PP in these reservoirs is 2.42 ± 1.65 g $O_2 \cdot m^{-2} \cdot d^{-1}$, ranging from 0.13 to 10.22 g $O_2 \cdot m^{-2} \cdot d^{-1}$, with a median of 2.15 g $O_2 \cdot m^{-2} \cdot d^{-1}$, indicating significant spatial variability. The YR basin exhibited the highest phytoplankton PP (3.54 ± 0.78 g $O_2 \cdot m^{-2} \cdot d^{-1}$), followed by the S/LR basin (3.25 ± 0.26 g $O_2 \cdot m^{-2} \cdot d^{-1}$) and the H/HR basin (3.07 ± 0.34 g $O_2 \cdot m^{-2} \cdot d^{-1}$) (Figure 3A). In contrast, the lowest phytoplankton PP values were observed in the NIR basin (0.45 ± 0. 16 g $O_2 \cdot m^{-2} \cdot d^{-1}$) and the SWR basin (0.99 ± 0.29 g $O_2 \cdot m^{-2} \cdot d^{-1}$). The YTZ basin and the PR basin recorded phytoplankton PP values of 2.18 ± 0.17 g $O_2 \cdot m^{-2} \cdot d^{-1}$ and 1.17 ± 0.28 g $O_2 \cdot m^{-2} \cdot d^{-1}$, respectively. The phytoplankton PP in the YR basin, S/LR basin, and H/HR basin was significantly higher than that in the PR basin, NIR basin, and SWR basin ($P < 0.05$).

Phytoplankton PP increased from small I-type (S1) to large I-type (L1) reservoirs but decreased in large II-type (L2) reservoirs (Figure 3B). The order of phytoplankton PP was as follows: L1 (3.46 ± 0.53 g $O_2 \cdot m^{-2} \cdot d^{-1}$) > M (2.36 ± 0.22 g $O_2 \cdot m^{-2} \cdot d^{-1}$) > S2 (2.18 ± 0.19 g $O_2 \cdot m^{-2} \cdot d^{-1}$) > S1 (2.12 ± 0.29 g $O_2 \cdot m^{-2} \cdot d^{-1}$) > L2 (2.10 ± 0.34 g $O_2 \cdot m^{-2} \cdot d^{-1}$). No significant difference in phytoplankton PP across reservoirs of various sizes.

3.2 Temporal variations of phytoplankton PP in Chinese reservoirs

The long-term series showed peak phytoplankton PP in the 1990s, subsequent decline, and recent recovery in the 2020s (Figure 4A). Mann-Kendall tests indicated no significant

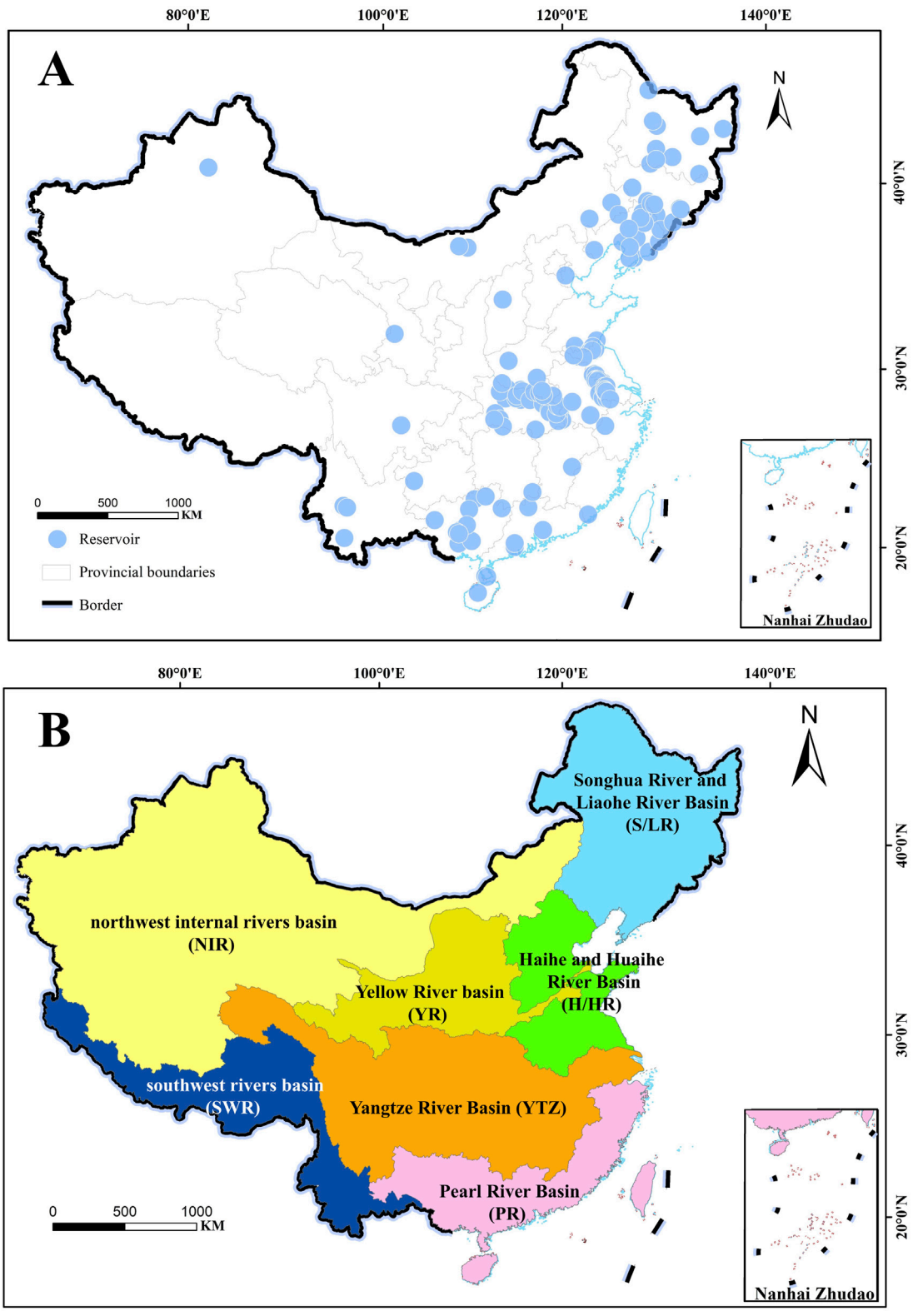

FIGURE 1
Reservoir distributions **(A)** and river basin divisions **(B)**. All reservoirs are categorized into seven major basins, including the Songhua River and Liaohe River (S/LR) basin, the Haihe and Huaihe River (H/HR) basin, the Yellow River (YR) basin, the Yangtze River (YTZ) basin, the Pearl River (PR) basin, the southwest rivers (SWR) basin and the northwest internal rivers (NIR) basin (Zhou et al., 2024). The Pearl River Basin includes the watersheds of the Southeast Rivers.

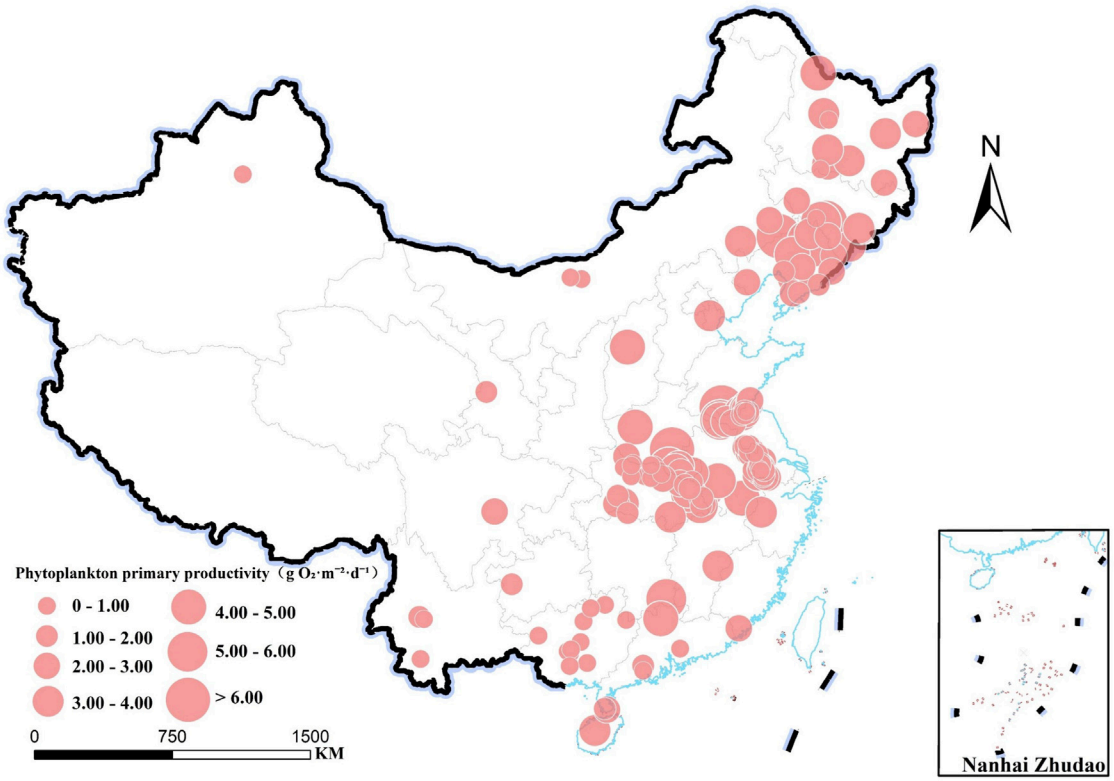

FIGURE 2
Spatial differentiation of phytoplankton PP in reservoirs across China.

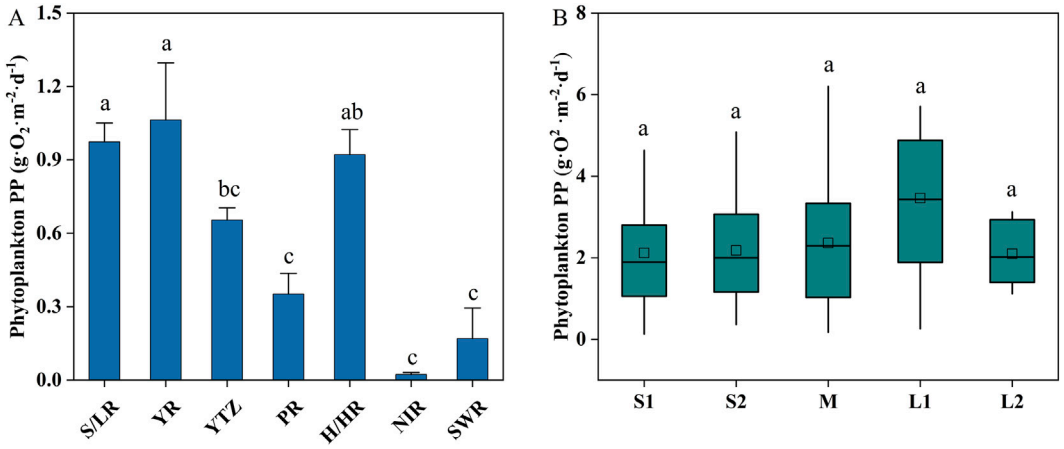

FIGURE 3
Spatial distribution characteristics of phytoplankton PP in reservoirs across China **(A)**. Variations in phytoplankton PP among reservoirs of different sizes **(B)**. S1 and S2 are small reservoirs with capacities less than 0.1×10^8 m^3, between 0.1×10^8 m^3 and 1.0×10^8 m^3, respectively (Zhou et al., 2024). M is medium reservoir capacities between 1.0×10^8 m^3 and 10×10^8 m^3 (Zhou et al., 2024). L1 and L2 are large reservoirs with capacities ranging from 10×10^8 m^3 to 100×10^8 m^3 and exceeding 100×10^8 m^3, respectively (Zhou et al., 2024). Different small letters indicate $P < 0.05$.

temporal trends (Figure 4B). The overall ranking of phytoplankton PP was as follows: 1990s (3.18 ± 0.33 g $O_2 \cdot m^{-2} \cdot d^{-1}$) >2020s (2.82 ± 0.54 g $O_2 \cdot m^{-2} \cdot d^{-1}$) >2000s (2.40 ± 0.16 g $O_2 \cdot m^{-2} \cdot d^{-1}$) >1980s (2.38 ± 0.20 g $O_2 \cdot m^{-2} \cdot d^{-1}$) >2010s (2.20 ± 0.61 g $O_2 \cdot m^{-2} \cdot d^{-1}$). Seasonally (Figure 4C), phytoplankton PP was significantly higher in summer (4.65 ± 0.52 g $O_2 \cdot m^{-2} \cdot d^{-1}$) compared to winter (1.41 ± 0.44 g $O_2 \cdot m^{-2} \cdot d^{-1}$) ($P < 0.05$), approximately 3.3 times that of winter. Phytoplankton PP slightly increased in spring (2.94 ± 0.50 g $O_2 \cdot m^{-2} \cdot d^{-1}$) compared to autumn (2.89 ± 0.66 g $O_2 \cdot m^{-2} \cdot d^{-1}$), but this difference was not statistically significant ($P > 0.05$).

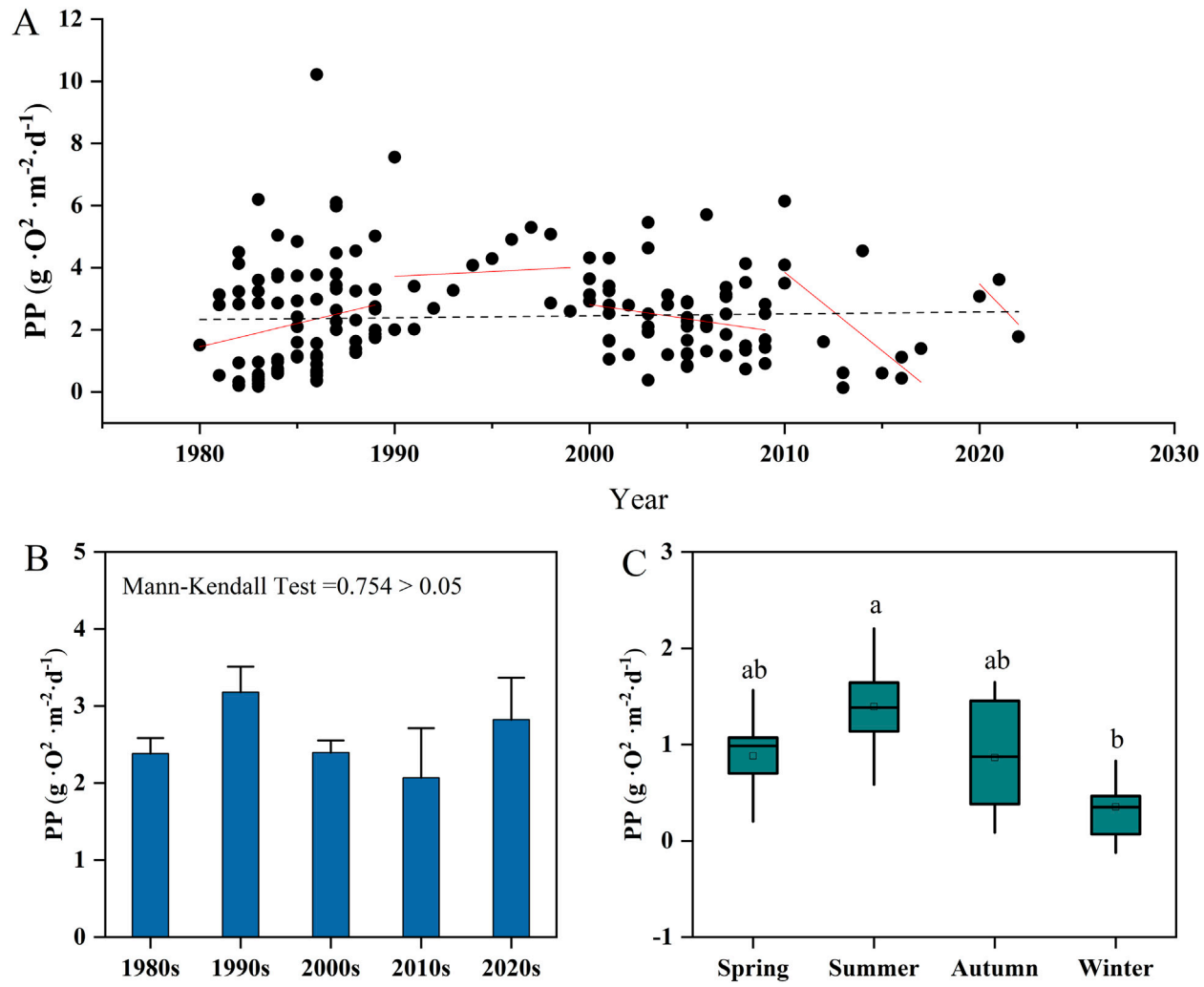

FIGURE 4
Temporal distribution characteristics of phytoplankton PP in reservoirs across China. **(A)** displays the distribution of PP data (1980–2023), with red and black trend lines representing decadal and full-period trends, respectively. **(B)** compares PP across time periods (mean ± SD; Mann-Kendall test). **(C)** shows seasonal variations in PP. Different small letters indicate significant differences at $P < 0.05$.

3.3 Influence of reservoir characteristics on phytoplankton PP in China

On the national scale, phytoplankton PP showed a weakly positive correlation with reservoir characteristics (Figure 5). None of the reservoir characteristics analyzed (including Secchi depth, total storage capacity, annual discharge, reservoir area, reservoir age, and retention time) were significantly correlated with phytoplankton PP ($P > 0.05$). Water depth was the only exception with a significant positive correlation with phytoplankton PP ($R = 0.17$, $P < 0.05$).

In basin-specific analyses (Table 2), phytoplankton PP demonstrated positive correlations with water depth in the PR basin ($R = 0.90$, $P < 0.01$) and the YTZ basin ($R = 0.28$, $P < 0.01$). Within the H/HR basin, there was a significant positive correlation between phytoplankton PP and reservoir area ($R = 0.68$, $P < 0.01$). However, no discernible correlations were observed between phytoplankton PP and parameters such as reservoir age, retention time, or annual discharge ($P > 0.05$).

3.4 Impact of nutrient and other characteristics on phytoplankton PP in China

Correlation analysis (Figure 6) reveals a significant positive correlation between phytoplankton PP and latitude alongside a significant negative correlation with average annual temperature and average annual rainfall ($P < 0.01$). Phytoplankton PP increases significantly with longitude, decreasing gradually from the east coast to the interior.

Phytoplankton PP demonstrated a significant positive correlation with TN and sunshine hours ($P < 0.01$) (Figure 6) but did not significantly correlate with TP (Supplementary Figure S1) or the N:P ratio ($P > 0.05$). However, at the basin-specific scale, this significant positive correlation between phytoplankton PP and TN was only observed in the YTZ basin ($P < 0.01$). In contrast, phytoplankton PP exhibited a significant positive correlation with the N:P ratio in the H/HR basin ($P < 0.01$). No significant correlation was identified between phytoplankton PP and TP across the river basins.

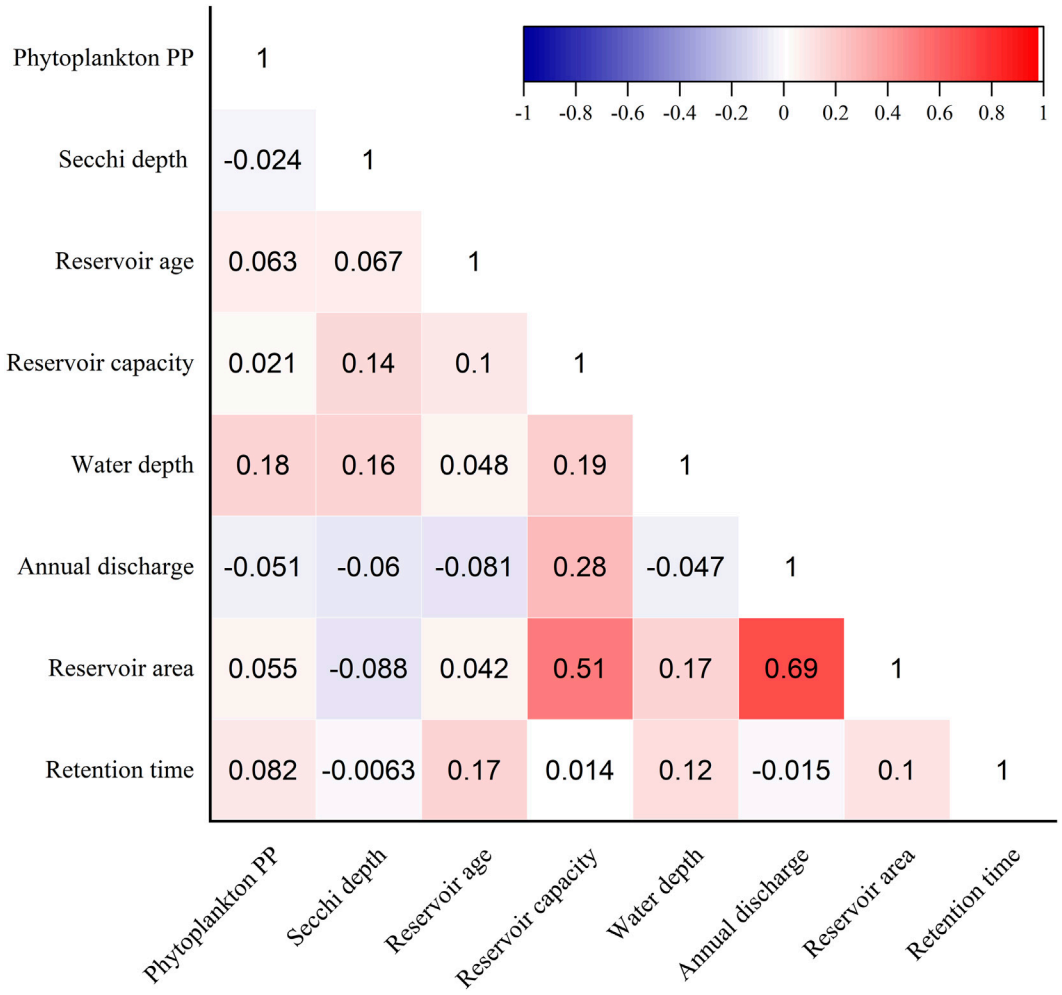

FIGURE 5
Correlation between phytoplankton PP and reservoir characteristics.

TABLE 2 Influence of reservoir characteristics on phytoplankton PP in different basin.

Factors	Phytoplankton PP			
	Haihe and Huaihe river basin	Yangtze river basin	Pearl river basin	Songhua river and Liaohe river basin
Secchi depth (cm)	−0.40*	NS	NS	NS
Water depth (m)	NS	0.27*	0.90**	NS
Reservoir area (km^2)	0.68**	NS	NS	NS
Total nitrogen ($mg{\cdot}L^{-1}$)	NS	0.33**	NS	NS
N:P ratio	0.66**	NS	NS	NS
Sunshine hours ($hours{\cdot}a^{-1}$)	0.76**	0.46**	0.68**	0.43*

NS, represents $P > 0.05$, *$P < 0.05$; **$P < 0.01$.

3.5 Estimation of total phytoplankton PP in Chinese reservoirs

The total phytoplankton PP in Chinese reservoirs was quantified as 22.08 $Tg{\cdot}O_2{\cdot}a^{-1}$. The YTZ basin leads in contribution, representing over 43% (9.55 $Tg{\cdot}O_2{\cdot}a^{-1}$) (Figure 7). The YR basin and the S/LR basin follow, contributing 21.67% (4.79 $Tg{\cdot}O_2{\cdot}a^{-1}$) and 21.46% (4.74 $Tg{\cdot}O_2{\cdot}a^{-1}$), respectively. The PR basin contributes 8.93% (1.97 $Tg{\cdot}O_2{\cdot}a^{-1}$). The NIR basin and SWR basin make more

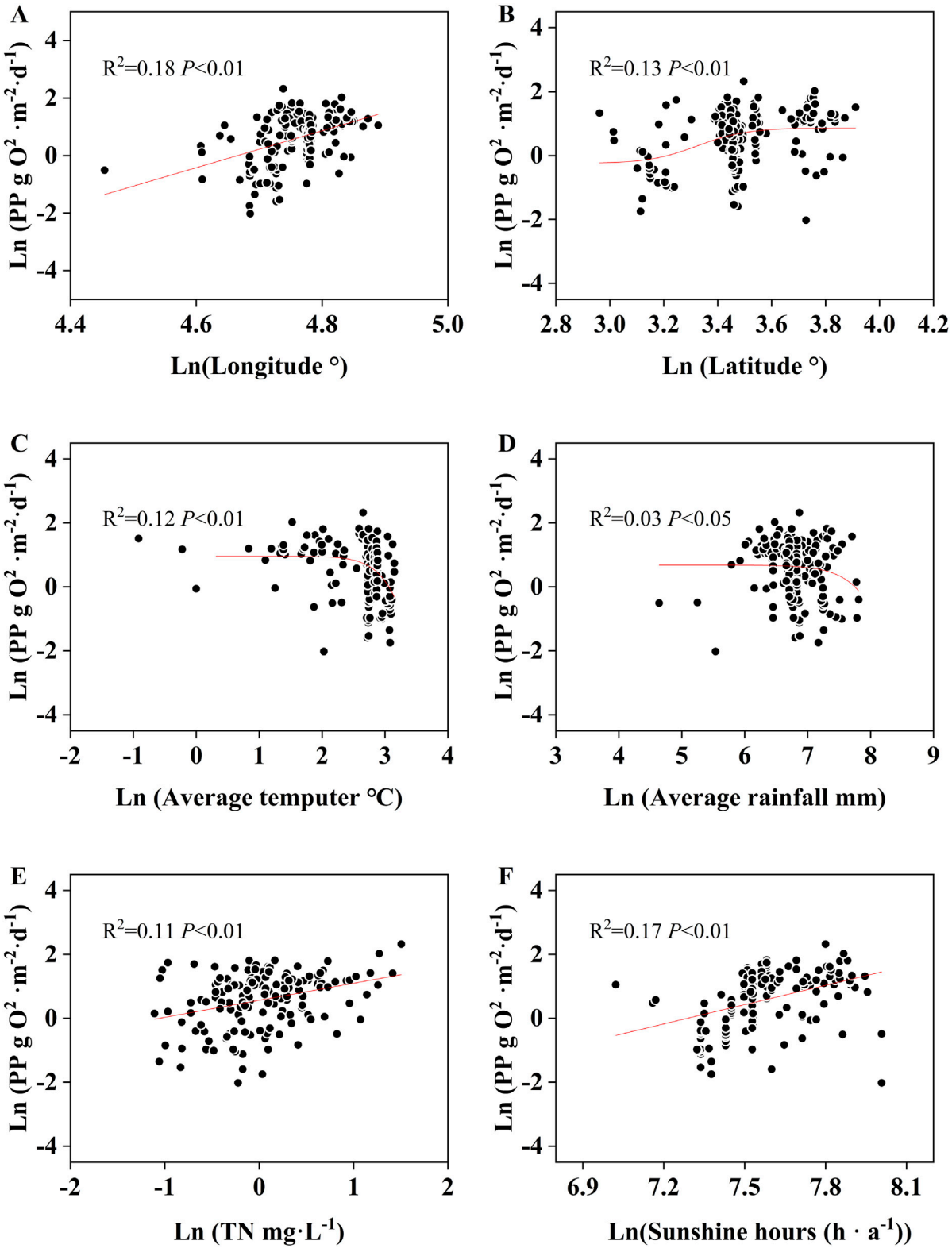

FIGURE 6
Correlation between phytoplankton PP and longitude **(A)**, latitude **(B)**, local annual average temperature **(C)**, annual rainfall **(D)**, TN **(E)** and sunshine hour **(F)** around the sample sites.

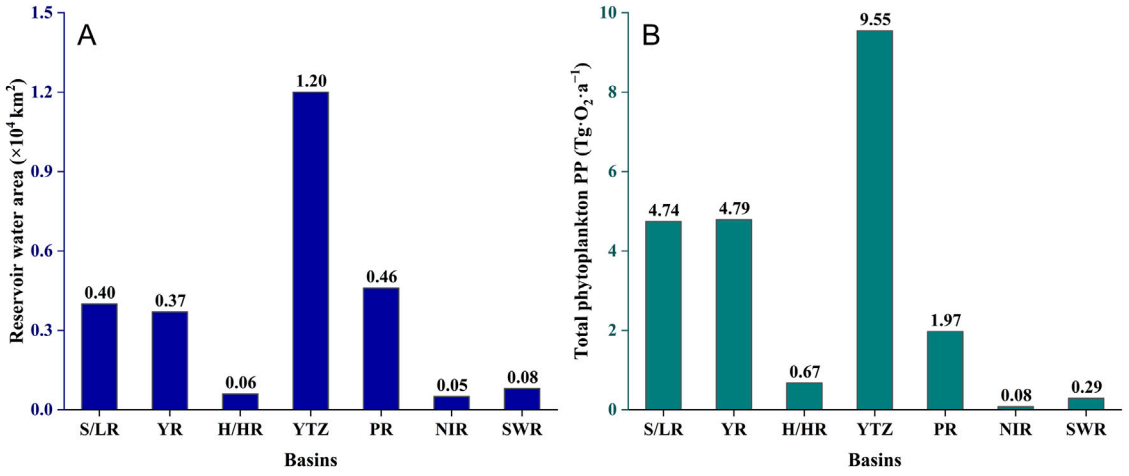

FIGURE 7
Estimation of total phytoplankton PP in different basins. **(A)** shows reservoir area, and **(B)** displays PP estimates.

modest contributions of 1.30% (0.29 $Tg{\cdot}O_2{\cdot}a^{-1}$) and 0.37% (0.08 $Tg{\cdot}O_2{\cdot}a^{-1}$), respectively.

4 Discussion

4.1 Factors influencing spatiotemporal variation of phytoplankton PP

Phytoplankton primary production (PP) shows significant latitudinal gradients across China's major basins, with higher values in the Yellow River (YR), Songhua River and Liaohe River (S/LR), and Haihe and Huaihe River (H/HR) basins compared to the Pearl River (PR), Northwest Internal Rivers (NIR), and Southwest Rivers (SWR) basins (Figure 3A). This south-north increasing trend reflects spatial variation in nutrient availability, light condition, and anthropogenic impacts (Wang et al., 2019b; Zhong et al., 2021; Jung et al., 2023). Eutrophic reservoirs in the eastern and northeastern plains sustain elevated PP through nutrient enrichment, whereas oligotrophic southwestern reservoirs with superior water quality limit growth due to nutrient scarcity (Yu et al., 2022; Hu et al., 2024). Extended growing seasons and favorable photoperiods enhance productivity in northern regions (Sun et al., 2023), while cloud cover and shorter photoperiods reduce output in PR and Yangtze (YTZ) basins (Ran et al., 2013a). Industrial activities in eastern/northeastern plains further alter productivity patterns via pollution loading (Cao et al., 2020). Topographic and climatic constraints render southwestern and Qinghai-Tibetan Plateau reservoirs particularly sensitive to temperature/precipitation variability (Ma et al., 2010).

Elevated phytoplankton PP in eastern plain reservoirs confirms established spatial eutrophication gradients, consistent with prior findings (Sun et al., 2023; Hu et al., 2024). Conversely, western regions (particularly Qinghai-Tibet Plateau and southwestern areas) exhibit nutrient-limited systems with suppressed PP (Deng et al., 2020).

Seasonal PP variations generally follow summer > spring > autumn > winter. While Sun et al. (2023) reported peak PP in spring/autumn for northern China (YTZ/SWR basins), this discrepancy likely stems from their predominant lake (vs. reservoir) sampling focus. Our reservoir data align with southern studies showing summer maxima > spring/autumn > winter (Ran et al., 2013a; Wang et al., 2019a; Yi et al., 2022). Dry-season reductions in nutrients and temperature constrain biomass and PP relative to wet periods (Lu et al., 2016). Notably, pronounced seasonal variability in downstream Yalongjiang and Three Gorges reservoirs underscore hydrological controls on PP dynamics (Ran et al., 2017a; 2017b; Deng et al., 2020).

4.2 Determinants of phytoplankton PP

Sixteen variables were analyzed to identify key drivers of phytoplankton PP in Chinese reservoirs. Sunshine hours, water depth, and rainfall emerged as primary predictors, though the stepwise regression model explained 28.9% of PP variation (Table 3). Regionally, the Yellow River (YR) and Songhua River and Liaohe River (S/LR) basins showed non-significant regression results. Significant drivers included: Sunshine hours and Reservoir capacity (explaining 70.0% variation) in the Haihe and Huaihe River (H/HR) basin; Sunshine hours and average rainfall (41.1%) in the Yangtze (YTZ) basin; water depth and reservoir area (89.5%) in Pearl River (PR) basin.

Phytoplankton photosynthetic rates exhibit a significant positive correlation with light radiation (Kirk, 1994). At the national scale, phytoplankton PP shows a significant positive correlation with sunshine hours ($r = 0.43$, $P < 0.01$), with stronger regional correlations ($r = 0.43–0.76$, $P < 0.01$). Rainfall constrains phytoplankton PP by reducing light availability, evidenced by significant negative correlations between light duration and rainfall, consistent with lower light duration in southwestern regions. Furthermore, turbidity and net radiation collectively regulate underwater light conditions (Sun et al., 2023): light intensity increases with radiation but decreases with turbidity (Tanabe et al., 2019). We used a light limitation index integrating Secchi depth and water depth, yet it showed no significant

TABLE 3 Multivariate linear regression model of phytoplankton PP.

Section	Model	R^2	Adjusted R^2	P Value
Nation	y = −9.645 + 0.002SH** + 0.03WD[a] + 0.001RF[a]	0.289	0.271	<0.001
H/HR basin	y = −12.165 + 0.008SH** + 0.191RC**	0.720	0.699	<0.001
YTZ basin	y = −4.924 + 0.002RF** + 0.003SH**	0.411	0.394	<0.001
PR basin	y = 0.766 + 0.086WD** − 0.10RA**	0.895	0.883	<0.001

[a]$P < 0.05$; **$P < 0.01$. H/HR, means the Haihe and Huaihe River basin; YTZ, basin means the Yangtze River (YTZ) basin, PR, basin means the Pearl River (PR) basin. SH, WD, RF, RC, and RA represent sunshine hours, water depth, rainfall, reservoir capacity, and reservoir area, respectively.

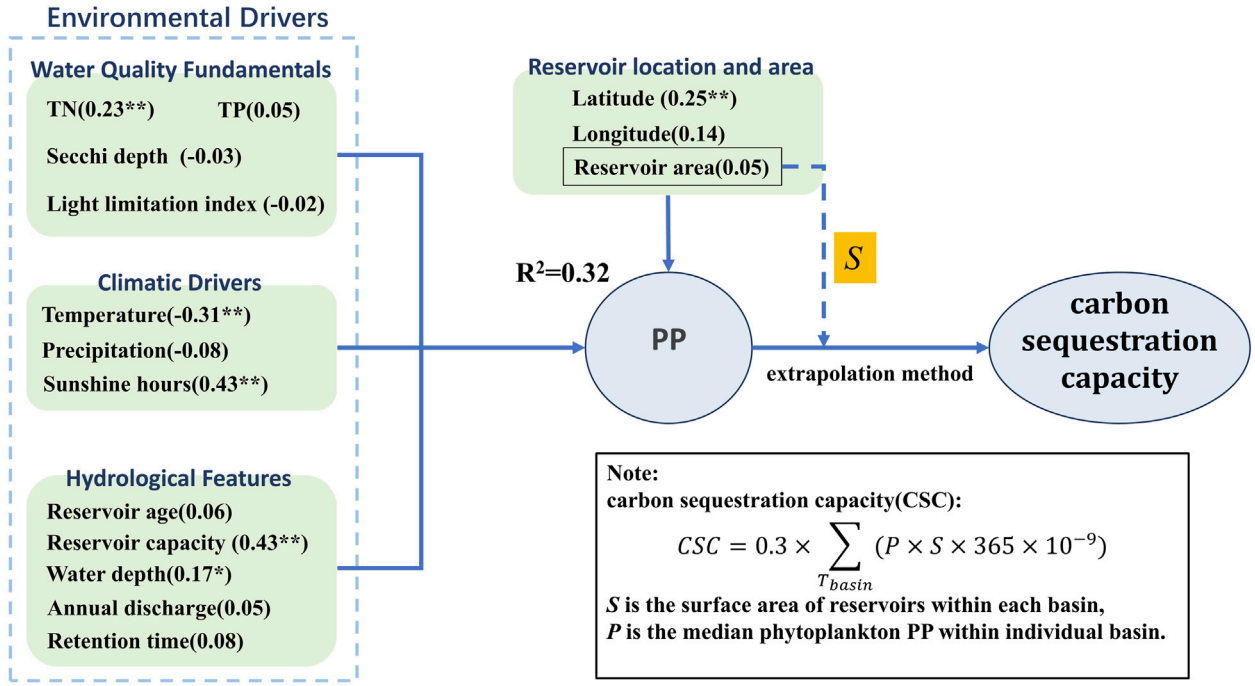

FIGURE 8
Conceptual framework linking drivers, phytoplankton PP and carbon sequestration. *$P < 0.05$; **$P < 0.01$.

correlation with phytoplankton PP (Supplementary Figure S1, $P > 0.05$). This contrasts with typical patterns where turbidity suppresses phytoplankton PP and light radiation enhances it. Consequently, the index's reliability as a phytoplankton PP indicator requires further validation, potentially influenced by limited sample size.

Nitrogen significantly influences PP in inland waters (Gao et al., 2019). In this study, the correlation between phytoplankton PP and TN is considerably stronger than between TP and phytoplankton PP, indicating nitrogen's critical limiting role. Phytoplankton PP significantly correlates with TN in the YTZ basin ($P < 0.05$). These findings contradict prior studies (Jia et al., 2022; Sun et al., 2023). Methodological differences may explain the divergence: model estimates versus field measurements, or combined lake-reservoir sampling increasing system heterogeneity. Among reservoir characteristics, only water depth shows a significant correlation with phytoplankton PP. This is because water depth critically influences light penetration, nutrient distribution, and thermal stratification, as established by previous studies (Ran et al., 2016; Wang et al., 2019a; Zhong et al., 2021; Jung et al., 2023). However, the regression model's limited predictive power suggests that key variables affecting phytoplankton PP in Chinese reservoirs remain unquantified or underexplored due to research constraints.

4.3 Carbon sequestration of phytoplankton in Chinese reservoirs

In addition to understanding the dynamics of PP, assessing the carbon sink capacity of reservoirs is critical (Figure 8). The total phytoplankton PP in Chinese reservoirs is 22.08 $Tg{\cdot}O_2{\cdot}a^{-1}$. Using the photosynthetic principle that 1 mg of O_2 release corresponds to 0.30 mg of organic carbon production (Shiying, 1981), the total carbon sequestration by phytoplankton in these reservoirs is estimated at 6.62 $Tg{\cdot}C{\cdot}a^{-1}$.

Previous studies estimate phytoplankton photosynthetic carbon sequestration in Chinese terrestrial aquatic ecosystems at approximately 18.69 and 19.41 $Tg{\cdot}C{\cdot}a^{-1}$, respectively (Gao et al., 2019; Sun et al., 2023). However, these studies did not differentiate

between lakes and reservoirs. Using the lake (75,703 km^2) and reservoir (25,616 km^2) area data from Sun et al. (2023), we recalculated the reservoir-specific carbon sequestration. This yielded estimates of 6.32 $Tg{\cdot}C{\cdot}a^{-1}$ based on Sun et al.'s total and 6.56 $Tg{\cdot}C{\cdot}a^{-1}$ based on Gao et al.'s total (Gao et al., 2019; Sun et al., 2023). These recalculated values closely align with this study's finding of 6.62 $Tg{\cdot}C{\cdot}a^{-1}$. Furthermore, compared to the global estimate for reservoir phytoplankton carbon sequestration (36 $Tg{\cdot}C{\cdot}a^{-1}$) (Maavara et al., 2017), the Chinese reservoir contribution represents 18.40% of the global total.

4.4 Uncertainty and limitations

Phytoplankton primary production estimation methods include light-dark bottle incubation, VGPM modeling, and carbon isotope techniques ($^{13}C/^{14}C$), deriving PP from dissolved oxygen changes, chlorophyll/environmental parameters, and carbonate isotopes, respectively (Pratt and Berkson, 1959; Cox et al., 2015; Lan et al., 2020; Lu et al., 2023). Methodological limitations and environmental factors cause significant PP discrepancies across methods or sites. Thus, this study exclusively uses light-dark bottle-sourced PP data to minimize methodological errors.

The light-dark bottle method exhibits broad applicability to river, reservoir, and estuary environments, with particular effectiveness in eutrophic waters. Key limitations include: (1) static incubation impeding nutrient replenishment in flowing waters, potentially causing PP underestimation; (2) exclusion of benthic metabolism, preventing comprehensive ecosystem assessment; and (3) reduced sensitivity in oligotrophic or high-bacterial-concentration waters (Hs et al., 2019; Loken et al., 2021; Molinari et al., 2021). This study employed the light-dark bottle method to measure reservoir phytoplankton PP. The method revealed low PP measurements in oligotrophic and mesotrophic reservoirs (Lu et al., 2023). Southern China's oligotrophic reservoirs, experiencing long-term nutrient deficiency, light limitation, thermal stratification, and other constraints, inherently exhibit low phytoplankton PP (Chen et al., 2020; Deng et al., 2020; Li et al., 2022). Consequently, the light-dark bottle method may underestimate PP and carbon sequestration potential in such systems. Furthermore, severe data gaps exist in some regions (e.g., only three reservoirs sampled each in each of the southwest river's basin and the northwest internal rivers basin), potentially limiting the model's explanatory power regarding driving factors. Seasonal data may also be biased since not all reservoirs include seasonal data.

This study investigates phytoplankton PP characteristics and carbon sequestration potential in Chinese reservoirs, revealing significant impacts of regional variations, seasonal fluctuations, and environmental factors (Sun et al., 2023; Wei et al., 2024). To advance the understanding of carbon balance dynamics in these ecosystems, future research must resolve these uncertainties. Implementing a comprehensive long-term monitoring system is therefore essential for systematic assessment of reservoir phytoplankton PP.

5 Conclusion

Phytoplankton primary production (PP) in Chinese reservoirs averaged 2.42 ± 1.65 g $O_2{\cdot}m^{-2}{\cdot}d^{-1}$ (range: 0.13–10.82). Spatially, PP was significantly elevated in the Yellow River (YR), Songhua River and Liaohe River (S/LR), and Haihe and Huaihe River (H/HR) basins relative to the Pearl River (PR), Northwest Internal Rivers (NIR), and Southwest Rivers (SWR) basins. Temporally, PP peaked in the 1990s (3.18 ± 0.33 g $O_2{\cdot}m^{-2}{\cdot}d^{-1}$), declined subsequently, and rebounded in the 2020s (2.82 ± 0.54 g $O_2{\cdot}m^{-2}{\cdot}d^{-1}$), with the full sequence being: 1990s > 2020s > 2000s (2.40 ± 0.16 g $O_2{\cdot}m^{-2}{\cdot}d^{-1}$) > 1980s (2.38 ± 0.20 g $O_2{\cdot}m^{-2}{\cdot}d^{-1}$) > 2010s (2.20 ± 0.61 g $O_2{\cdot}m^{-2}{\cdot}d^{-1}$). Seasonal maxima occurred in summer (4.65 ± 0.52 g $O_2{\cdot}m^{-2}{\cdot}d^{-1}$) and minima in winter (1.41 ± 0.44 g $O_2{\cdot}m^{-2}{\cdot}d^{-1}$). A multivariate linear regression identified sunshine hours, water depth, and rainfall as the strongest predictors of PP, collectively accounting for 28.9% of the observed variance. Extrapolation yielded an annual reservoir PP of 22.08 $Tg{\cdot}O_2{\cdot}a^{-1}$, dominated by the Yangtze basin. This represents 6.62 $Tg{\cdot}C{\cdot}a^{-1}$ of carbon sequestration—18.40% of the global reservoir estimate (36 Tg C a^{-1}). Our analysis delineates spatio-temporal patterns of phytoplankton PP in Chinese reservoirs and underscores its significance for regional carbon budgets, aquatic ecosystem dynamics, and sustainable resource management.

Data availability statement

The original contributions presented in the study are included in the article/Supplementary Material, further inquiries can be directed to the corresponding author.

Author contributions

HD: Conceptualization, Visualization, Formal Analysis, Software, Methodology, Data curation, Writing – original draft, Writing – review and editing, Validation, Investigation, Funding acquisition. ZZ: Funding acquisition, Resources, Writing – review and editing, Project administration, Conceptualization. QC: Conceptualization, Data curation, Writing – review and editing. JW: Software, Writing – review and editing, Data curation. AC: Writing – review and editing, Funding acquisition, Supervision, Validation.

Funding

The author(s) declare that financial support was received for the research and/or publication of this article. This research was funded by the National Natural Science Foundation of China (No. 42401044 and 42301128), the High-Level Project Cultivation Plan of Zhaoqing University (No. GCCZK202413), and the Zhaoqing University Scientific Research Fund Project (No. QN202231), the Natural Science Key Research Project of Universities in Anhui Province (No. 2022AH051672).

Conflict of interest

The authors declare that the research was conducted in the absence of any commercial or financial relationships that could be construed as a potential conflict of interest.

Generative AI statement

The author(s) declare that no Generative AI was used in the creation of this manuscript.

Any alternative text (alt text) provided alongside figures in this article has been generated by Frontiers with the support of artificial intelligence and reasonable efforts have been made to ensure accuracy, including review by the authors wherever possible. If you identify any issues, please contact us.

Publisher's note

Supplementary material

The Supplementary Material for this article can be found online at: https://www.frontiersin.org/articles/10.3389/fenvs.2025.1615267/full#supplementary-material

References

Berga, L., Buil, J. M., Bofill, E., De Cea, J. C., Garcia Perez, J. A., Mañueco, G., et al. (2006). *Dams and reservoirs, societies and environment in the 21st century*. London: Taylor and Francis Group Two Volume Set. doi:10.1201/b16818

Cao, Z., Ma, R., Duan, H., Pahlevan, N., Melack, J., Shen, M., et al. (2020). A machine learning approach to estimate chlorophyll-a from Landsat-8 measurements in inland lakes. *Remote Sens. Environ.* 248, 111974. doi:10.1016/j.rse.2020.111974

Carey, J. C., and Fulweiler, R. W. (2012). Human activities directly alter watershed dissolved silica fluxes. *Biogeochemistry* 111, 125–138. doi:10.1007/s10533-011-9671-2

Chen, Q., Shi, W., Huisman, J., Maberly, S. C., Zhang, J., Yu, J., et al. (2020). Hydropower reservoirs on the upper Mekong River modify nutrient bioavailability downstream. *Natl. Sci. Rev.* 7, 1449–1457. doi:10.1093/nsr/nwaa026

Cox, T. J. S., Maris, T., Soetaert, K., Kromkamp, J. C., Meire, P., and Meysman, F. (2015). Estimating primary production from oxygen time series: a novel approach in the frequency domain. *Limnol. Oceanogr. Methods* 13, 529–552. doi:10.1002/lom3.10046

Deng, H., Tao, Z., Gao, Q., Yao, L., Feng, Y., Li, Y., et al. (2020). Variation of biogeochemical cycle of riverine dissolved inorganic carbon and silicon with the cascade damming. *Environ. Sci. Pollut. Res.* 27, 28840–28852. doi:10.1007/s11356-020-09174-5

Essa, D. I., Elshobary, M. E., Attiah, A. M., Salem, Z. E., Keshta, A. E., and Edokpayi, J. N. (2024). Assessing phytoplankton populations and their relation to water parameters as early alerts and biological indicators of the aquatic pollution. *Ecol. Indic.* 159, 111721. doi:10.1016/j.ecolind.2024.111721

Gao, Y., Ma, M., Yang, T., Chen, W., and Yang, T. (2018). Global atmospheric sulfur deposition and associated impaction on nitrogen cycling in ecosystems. *J. Clean. Prod.* 195, 1–9. doi:10.1016/j.jclepro.2018.05.166

Gao, Y., Jia, Y., Yu, G., He, N., Zhang, L., Zhu, B., et al. (2019). Anthropogenic reactive nitrogen deposition and associated nutrient limitation effect on gross primary productivity in inland water of China. *J. Clean. Prod.* 208, 530–540. doi:10.1016/j.jclepro.2018.10.137

Gao, Y., Jia, J., Lu, Y., Yang, T., Lyu, S., Shi, K., et al. (2021). Determining dominating control mechanisms of inland water carbon cycling processes and associated gross primary productivity on regional and global scales. *Earth-Science Rev.* 213, 103497. doi:10.1016/j.earscirev.2020.103497

Grill, G., Lehner, B., Thieme, M., Geenen, B., Tickner, D., Antonelli, F., et al. (2019). Mapping the world's free-flowing rivers. *Nature* 569, 215–221. doi:10.1038/s41586-019-1111-9

Han, Q., Wang, B., Liu, C. Q., Wang, F., Peng, X., and Liu, X. L. (2018). Carbon biogeochemical cycle is enhanced by damming in a karst river. *Sci. Total Environ.* 616–617, 1181–1189. doi:10.1016/j.scitotenv.2017.10.202

Hiroki, M., Tomioka, N., Murata, T., Imai, A., Jutagate, T., Preecha, C., et al. (2020). Primary production estimated for large lakes and reservoirs in the Mekong River Basin. *Sci. Total Environ.* 747, 141133. doi:10.1016/j.scitotenv.2020.141133

Ho, J. C., Michalak, A. M., and Pahlevan, N. (2019). Widespread global increase in intense lake phytoplankton blooms since the 1980s. *Nature* 574, 667–670. doi:10.1038/s41586-019-1648-7

Hs, P. J., Daggula, N., Maloth, M., Praveen, C., Hs, J., Naik, R., et al. (2019). Primary productivity and phytoplankton diversity in Pilikula Lake, Dakshina Kannada dist, Karnataka, India. *J. Entomol. Zool. Stud.* 7, 133–139.

Hu, M., Ma, R., Xue, K., Cao, Z., Xiong, J., Loiselle, S. A., et al. (2024). Eutrophication evolution of lakes in China: four decades of observations from space. *J. Hazard. Mater.* 470, 134225. doi:10.1016/j.jhazmat.2024.134225

Hughes, H. J., Bouillon, S., André, L., and Cardinal, D. (2012). The effects of weathering variability and anthropogenic pressures upon silicon cycling in an intertropical watershed (Tana River, Kenya). *Chem. Geol.* 308–309, 18–25. doi:10.1016/j.chemgeo.2012.03.016

Jia, J., Gao, Y., Zhou, F., Shi, K., Johnes, P. J., Dungait, J. A. J., et al. (2020). Identifying the main drivers of change of phytoplankton community structure and gross primary productivity in a river-lake system. *J. Hydrol.* 583, 124633. doi:10.1016/j.jhydrol.2020.124633

Jia, J., Gao, Y., Sun, K., Lu, Y., Wang, J., and Shi, K. (2022). Phytoplankton community composition, carbon sequestration, and associated regulatory mechanisms in a floodplain lake system. *Environ. Pollut.* 306, 119411. doi:10.1016/j.envpol.2022.119411

Jia, J., Dungait, J. A. J., Lu, Y., Cui, T., Yu, G., and Gao, Y. (2023). Inland water metabolic carbon processes and associated biological mechanisms that drive carbon source-sink instability. *Innov. Geosci.* 1, 100035. doi:10.59717/j.xinn-geo.2023.100035

Jung, E., Joo, G. J., Kim, H. G., Kim, D. K., and Kim, H. W. (2023). Effects of seasonal and diel variations in thermal stratification on phytoplankton in a regulated river. *Sustainability* 15, 16330. doi:10.3390/su152316330

Kirk, J. T. O. (1994). *Light and photosynthesis in aquatic ecosystems*. 2nd edn. doi:10.2307/2405114

Lan, K. W., Lian, L. J., Li, C. H., Hsiao, P. Y., and Cheng, S. Y. (2020). Validation of a primary production algorithm of vertically generalized production model derived from multi-satellite data around the waters of Taiwan. *Remote Sens.* 12, 1627. doi:10.3390/rs12101627

Lehner, B., Liermann, C. R., Revenga, C., Vörömsmarty, C., Fekete, B., Crouzet, P., et al. (2011). High-resolution mapping of the world's reservoirs and dams for sustainable river-flow management. *Front. Ecol. Environ.* 9, 494–502. doi:10.1890/100125

Li, J., Pu, J., and Zhang, T. (2022). Transport and transformation of dissolved inorganic carbon in a subtropical groundwater-fed reservoir, south China. *Water Res.* 209, 117905. doi:10.1016/j.watres.2021.117905

Loken, L. C., Van Nieuwenhuyse, E. E., Dahlgren, R. A., Lenoch, L. E. K., Stumpner, P. R., Burau, J. R., et al. (2021). Assessment of multiple ecosystem metabolism methods in an estuary. *Limnol. Oceanogr. Methods* 19, 741–757. doi:10.1002/lom3.10458

Lu, T., Chen, N., Duan, S., Chen, Z., and Huang, B. (2016). Hydrological controls on cascade reservoirs regulating phosphorus retention and downriver fluxes. *Environ. Sci. Pollut. Res.* 23, 24166–24177. doi:10.1007/s11356-016-7397-3

Lu, Y., Huang, L., Jia, J., and Gao, Y. (2023). Estimation of primary productivity of inland water. *Adv. Earth Sci.* 38, 57–69. doi:10.11867/j.issn.1001-8166.2022.055

Ma, R., Duan, H., Hu, C., Feng, X., Li, A., Ju, W., et al. (2010). A half-century of changes in China's lakes: global warming or human influence? *Geophys. Res. Lett.* 37, L24106. doi:10.1029/2010GL045514

Maavara, T., Lauerwald, R., Regnier, P., and Van Cappellen, P. (2017). Global perturbation of organic carbon cycling by river damming. *Nat. Commun.* 8, 15347. doi:10.1038/ncomms15347

Molinari, B., Stewart-Koster, B., Adame, M. F., Campbell, M. D., McGregor, G., Schulz, C., et al. (2021). Relationships between algal primary productivity and environmental variables in tropical floodplain wetlands. *Inl. Waters* 11, 180–190. doi:10.1080/20442041.2020.1843932

Pratt, D. M., and Berkson, H. (1959). Two sources of error in the oxygen light and dark bottle method. *Limnol. Oceanogr.* 4, 328–334. doi:10.4319/lo.1959.4.3.0328

Ran, X., Yu, Z., Chen, H., Zhang, X., and Guo, H. (2013a). Silicon and sediment transport of the changjiang river (Yangtze River): could the three Gorges reservoir be a filter? *Environ. Earth Sci.* 70, 1881–1893. doi:10.1007/s12665-013-2275-5

Ran, X., Yu, Z., Yao, Q., Chen, H., and Guo, H. (2013b). Silica retention in the three Gorges reservoir. *Biogeochemistry* 112, 209–228. doi:10.1007/s10533-012-9717-0

Ran, X., Liu, S., Liu, J., Zang, J., Che, H., Ma, Y., et al. (2016). Composition and variability in the export of biogenic silica in the changjiang River and the effect of three Gorges reservoir. *Sci. Total Environ.* 571, 1191–1199. doi:10.1016/j.scitotenv.2016.07.125

Ran, X., Bouwman, L., Yu, Z., Beusen, A., Chen, H., and Yao, Q. (2017a). Nitrogen transport, transformation, and retention in the Three Gorges Reservoir: a mass balance approach. *Limnol. Oceanogr.* 62, 2323–2337. doi:10.1002/lno.10568

Ran, X., Xu, B., Liu, J., Zhao, C., Liu, S., and Zang, J. (2017b). Biogenic silica composition and δ13C abundance in the Changjiang (Yangtze) and Huanghe (Yellow) Rivers with implications for the silicon cycle. *Sci. Total Environ.* 579, 1541–1549. doi:10.1016/j.scitotenv.2016.11.161

Ran, L., Butman, D. E., Battin, T. J., Yang, X., Tian, M., Duvert, C., et al. (2021). Substantial decrease in CO2 emissions from Chinese inland waters due to global change. *Nat. Commun.* 12, 1730–1739. doi:10.1038/s41467-021-21926-6

Ruan, Q., Liu, H., Dai, Z., Wang, F., and Cao, W. (2024). Damming exacerbates the discontinuities of phytoplankton in a subtropical river in China. *J. Environ. Manage.* 351, 119832. doi:10.1016/j.jenvman.2023.119832

Rusanov, A. G., Bíró, T., Kiss, K. T., Buczkó, K., Grigorszky, I., Hidas, A., et al. (2022). Relative importance of climate and spatial processes in shaping species composition, functional structure and beta diversity of phytoplankton in a large river. *Sci. Total Environ.* 807, 150891. doi:10.1016/j.scitotenv.2021.150891

Shiying, L. (1981). The results of the conversion of primary productivity. *Freshw. Fish.* 1, 30–31.

Sun, K., Deng, W., Jia, J., and Gao, Y. (2023). Spatiotemporal patterns and drivers of phytoplankton primary productivity in China's lakes and reservoirs at a national scale. *Glob. Planet. Change* 228, 104215. doi:10.1016/j.gloplacha.2023.104215

Tanabe, Y., Hori, M., Mizuno, A. N., Osono, T., Uchida, M., Kudoh, S., et al. (2019). Light quality determines primary production in nutrient-poor small lakes. *Sci. Rep.* 9, 4639. doi:10.1038/s41598-019-41003-9

Wagner, T., and Erickson, L. E. (2017). Sustainable management of eutrophic lakes and reservoirs. *J. Environ. Prot. Irvine, Calif.* 08 (08), 436–463. doi:10.4236/jep.2017.84032

Wang, W., Li, S. L., Zhong, J., Li, C., Yi, Y., Chen, S., et al. (2019a). Understanding transport and transformation of dissolved inorganic carbon (DIC)in the reservoir system using δ13CDIC and water chemistry. *J. Hydrol.* 574, 193–201. doi:10.1016/j.jhydrol.2019.04.036

Wang, W., Li, S., Zhong, J., Maberly, S. C., Li, C., Wang, F., et al. (2019b). Climatic and anthropogenic regulation of carbon transport and transformation in a karst river-reservoir system. *Sci. Total Environ.* 707, 135628. doi:10.1016/j.scitotenv.2019.135628

Wang, Y., Gu, D., Liu, Z., Lu, J., Hu, T., Li, G., et al. (2024). Characteristics and impacts of pollution and remediation on riverine greenhouse gas emissions: a review. *Sustainability* 16, 11061. doi:10.3390/su162411061

Wei, J., Ji, X., and Hu, W. (2022). Characteristics of phytoplankton production in wet and dry seasons in hyper-eutrophic lake taihu, China. *Sustainability* 14, 11216. doi:10.3390/su141811216

Wei, J., Ji, X., and Hu, W. (2024). Characteristics of phytoplankton productivity in three typical lake zones of Taihu, China. *Sustainability* 16, 2376. doi:10.3390/su16062376

Xiao, L. J., Zhu, Y., Yang, Y., Lin, Q., Han, B. P., and Padisák, J. (2018). Species-based classification reveals spatial processes of phytoplankton meta-communities better than functional group approaches: a case study from three freshwater lake regions in China. *Hydrobiologia* 811, 313–324. doi:10.1007/s10750-017-3502-y

Yi, Y., Li, S. L., Zhong, J., Wang, W., Chen, S., Bao, H., et al. (2022). The influence of the deep subtropical reservoir on the karstic riverine carbon cycle and its regulatory factors: insights from the seasonal and hydrological changes. *Water Res.* 226, 119267. doi:10.1016/j.watres.2022.119267

Yu, H., Shi, X., Zhao, S., Sun, B., Liu, Y., Arvola, L., et al. (2022). Primary productivity of phytoplankton and its influencing factors in cold and arid regions: a case study of Wuliangsuhai Lake, China. *Ecol. Indic.* 144, 109545. doi:10.1016/j.ecolind.2022.109545

Zhang, M., Yu, Y., Yang, Z., and Kong, F. (2016). Deterministic diversity changes in freshwater phytoplankton in the Yunnan-Guizhou Plateau lakes in China. *Ecol. Indic.* 63, 273–281. doi:10.1016/j.ecolind.2015.12.017

Zhong, J., Wallin, M. B., Wang, W., Li, S. L., Guo, L., Dong, K., et al. (2021). Synchronous evaporation and aquatic primary production in tropical river networks. *Water Res.* 200, 117272–117279. doi:10.1016/j.watres.2021.117272

Zhou, T., Wang, X., Xiao, Z., Qing, Z., Li, X., Wang, J., et al. (2024). Characteristics and influencing factors of CO2 emission from inland waters in China. *Sci. China Earth Sci.* 67, 2034–2055. doi:10.1007/s11430-023-1286-5